RMBK SP-2 Validation Results (KS PH Rupture Simulation)

Bruce Schmitt
Battelle, PNNL

ABSTRACT

The RELAP5 code has been developed for best estimate transient simulations of light water reactor coolant systems, during postulated accidents. Although developed and tested primarily for typical Western PWR and BWR reactor designs, the code is also being applied to safety assessments of Russian-designed reactors (RBMK and VVER reactors). With the assistance of the United States Department of Energy (USDOE), through the Department's International Nuclear Safety Program, a project was established with the Russian International Nuclear Safety Center (RINSC) to address validation issues of the RELAP5 code. Through RINSC, with the participation of multiple Russian organizations, a process was initiated to identify and prioritize transient phenomena and experimental facilities with the purpose of defining standard problems that could be used to validate the RELAP5 code for application to RBMK and VVER reactors.

RBMK Standard Problem 2 (SP2) was defined from a series of stop flow experiments that were performed with the KS facility. The KS facility is an electrically heated full-scale mockup of an RBMK fuel channel. The SP2 tests were designed to simulate the RBMK design-basis accident of a large header rupture at full power and flow. That is, to simulate the abrupt flow stoppage that would occur following a rupture, and then the subsequent quenching when flow is re-established. The results of the analysis for SP2 indicated that RELAP5 provided minimal or poor agreement with the test data. The primary discrepancy was seen with the heater rod quench after flow was re-established. However, significant discrepancies were also seen with the steady state initialization for the differential pressure of the heater region.

This report is an extension of the SP2 analysis and investigates the discrepancies seen in the steady-state initialization for the heater bundle two-phase differential pressure. The VIPRE-01 code was used as a code-to-code comparison for the steady state solution to investigate whether sub-channel effects could be a significant issue, and also to compare different two-phase multipliers. Within VIPRE-01 the EPRI and Beattie two-phase multipliers were investigated. In addition, different two-phase multipliers were investigated within the RELAP5 code (beyond the default HTFS model). These included the Friedal, EPRI and Beattie correlations, as well as a simplified multiplier based on the sonic velocity of the two-phase mixture. RBMK Standard Problem 1 (SP1) was also re-evaluated. SP1 was a series of stop flow experiments performed with the KS facility to simulate an abrupt flow stoppage under low thermal loads. These experiments were performed to investigate counter-current flow phenomenon under low thermal loads. The SP1 evaluation results had shown slightly better agreement than the SP2 results, however, the results had also shown significant discrepancies for the steady state bundle two-phase pressure drop.

INTRODUCTION

The RELAP5 code has been developed for best estimate transient simulations of light water reactor coolant systems, during postulated accidents. Although developed and tested primarily for typical Western PWR and BWR reactor designs, the code is also being applied to safety assessments of Russian-designed reactors (RBMK and VVER reactors). With the assistance of the United States Department of Energy (USDOE), through the Department's International Nuclear Safety Program (INSP), a project was established with the Russian International Nuclear Safety Center (RINSC) to address validation issues of the RELAP5 code. Through RINSC, with the participation of multiple Russian organizations, a process was initiated to identify and prioritize transient phenomena and experimental facilities with the purpose of defining standard problems that could be used to validate the RELAP5 code for application to RBMK and VVER reactors. The code version used in this program has been RELAP5/MOD3.2 [1].

This report is an extension of the RBMK Standard Problem 2 (SP2) analysis [2] and investigates the discrepancies seen in the steady-state initialization for the heater bundle two-phase differential pressure. The VIPRE-01 code [3] was used as a code-to-code comparison for the steady state solution to investigate whether sub-channel effects could be a significant issue, and also to compare different two-phase multipliers. Within VIPRE-01 the EPRI and Beattie two-phase multipliers were investigated. In addition, different two-phase multipliers were investigated within the RELAP5 code (beyond the default HTFS model). These included the Friedal [4], EPRI and Beattie correlations (as coded in VIPRE-01), as well as a simplified multiplier based on the sonic velocity of the two-phase mixture. RBMK Standard Problem 1 (SP1) was also re-evaluated for the steady state heater bundle pressure drop.

SP2 was defined from a series of stop flow experiments that were performed with the KS facility to simulate the abrupt flow stoppage in the fuel channel (FC) that would occur following a header rupture. Six of these experiments were selected for evaluation ranging in heater power from 1.69MWth to 4.56MWth, with various initial coolant inlet temperatures, inlet flow rates and system pressures. The initial conditions for each test are given in Table 1 below. Five of the experiments were performed with constant heater power and one experiment was performed with a variable power. Test-8 did not provide a bundle differential pressure measurement (due to instrumentation failure), and so it is not included in this additional evaluation. The primary effort of the original study was to evaluate the ability of RELAP5 to calculate rod bundle dryout and/or burn-out (critical heat flux) following the stoppage of flow and the subsequent rewetting after the flow was restored.

Table 1) SP2 Initial Conditions

Case	Power (MWth)	Channel inlet pressure (Mpa)	Coolant inlet temperature (K)	Mass flow / flux (kg/s) / (kg/m2-s)	Bundle pressure drop (Pa)
Test-4	1.691	7.68	516.1	3.90 / 1716	183,100
Test-5	2.486	8.40	527.4	4.70 / 2068	261,600
Test-5'	2.532	7.95	533.1	4.17 / 1835	271,500
Test-6	2.926	8.23	527.3	4.28 / 1883	271,400
Test-7	3.488	8.23	529.3	4.13 / 1830	310,700
Test-8	4.566	8.74	531.1	6.27 / 2758	-

SP1 was defined from a series of stop flow experiments that were performed with the KS facility to simulate counter-current flow and dryout under low thermal loads and flow [5,6]. Nine of these experiments had been selected for evaluation ranging in heater power from 96kWth to 257kWth, with various initial coolant inlet temperatures, inlet flow rates and system pressures. The initial conditions for each test are given in Table 2 below. The primary effort of the original study was to investigate counter-current flow and dryout under low thermal loads and flow.

Table 2) SP1 Initial Conditions

Case	Power (KWth)	Channel inlet pressure (Mpa)	Coolant inlet temperature (K)	Mass flow / flux (kg/s) / (kg/m2-s)	Bundle pressure drop (Pa)
SF-96	96.2	4.72	515	0.583 / 277.1	52,400
SF-108	108.1	6.78	539	0.525 / 249.5	47,000
SF-128	128.6	6.78	537	0.516 / 245.3	45,000
SF-155	155.0	6.59	537	0.539 / 256.2	44,100
SF-161	161.0	4.91	514	0.583 / 277.1	49,500
SF-201	201.0	7.52	532	0.525 / 249.5	45,500
SF-202	201.5	5.12	507	0.566 / 269.0	51,900
SF-251	251.0	7.86	538	0.533 / 253.3	43,100
SF-257	257.0	5.19	515	0.564 / 268.1	47,500

FACILITY and MODEL DESCRIPTION

The KS facility schematic is shown in Figure 1. The KS circuit simulates of the main structural elements of the RBMK reactor. From Figure 3, the main heater section used was 'Test Section 2', and the main flow path lines have been 'bolded'. The facility includes a distribution header (Lower header) and lower water communication line with an isolating control valve (2p). This piping connects to a heated channel (Test section 2), which contains an electrically heated bundle assembly. For SP2 the heater bundle is an 18-pin assembly, and is surrounded by a talkoclorite insulator contained within the pressure tube. For SP1 the heater bundle is a 36-pin assembly, also surrounded by a talkoclorite insulator contained within the pressure tube. A riser with an internal shield plug, also called a lifting path, connects to the steam water communication (SWC) line leading to an upper header. A bypass line connecting the Lower and Upper headers, with control valve (4), effectively maintains constant differential pressure across the test section, even after inlet valve closure (2p). A more detailed description of the KS facility can be found in the definition report for SP2 [7].

Standard Problem 2

Figure 2 provides a simplified view of Test Section 2 between the Lower and Upper headers specific to SP2. Figure 3 provides the heater bundle detailed view, and Figure 4 the heater bundle cross-section view. The heater section is 7.0m in length and simulates an RBMK-1500 18-pin bundle. Full channel grid spacers are provided at 360mm intervals in both the upper and lower bundle regions. In the upper bundle half (3.5-7.0m) the grid spacer loss coefficient is given as k=0.91. In the lower bundle half (0-3.5m) the spacer loss is given as k=0.55. Partial grid spacers are provided in the upper bundle region between the full spacers (2 partial spacers at 120mm intervals). Their loss is given as k=0.28. Inlet mass flow, pressure and coolant temperature were

monitored in each experiment. In addition, the bundle differential pressure measurement is monitored across the full heater bundle length (DP16-4 in Figure 2).

The SP2 RELAP5 model simulated the entire KS facility, Figure 5. However, this study was interested only in the heater bundle region differential pressure response and so the remaining portions of the model are not described here. The model of the heater bundle used 58 axial nodes at 120mm lengths. This was a convenient split primarily done to try and capture the effects of the grid spacers for CHF and reflood in the original analysis. The axial power profile for each experiment was flat (1.0) across the bundle length. The radial pin power distribution was 0.88 for each of the inner 6-pins and 1.08 for each of the outer 12 pins, Figure 4. The heater pins were modeled as two rings of 6 and 12 pins to capture the radial power distribution.

Standard Problem 1

Figure 6 provides a simplified view of Test Section 2 between the Lower and Upper headers specific to SP1. Figure 7 provides the heater bundle detailed view, and Figure 8 the heater bundle cross-section view. The heater section is 6.0m in length and simulates an advanced RBMK 36-pin bundle design. Full channel grid spacers are provided at 250mm intervals along the entire bundle length. Their loss coefficient is given as k=0.55. Inlet mass flow, pressure and coolant temperature were monitored in each experiment. In addition, the bundle differential pressure measurement is monitored across the full heater bundle length (DP16-4 in Figure 6).

The SP1 RELAP5 model simulated only the region between the upper and lower headers, Figure 9. The model of the heater bundle used 24 axial nodes split at 250mm. Again, this was a convenient split to try and capture the effects of the grid spacers for CHF (these experiments did not include reflood data). The axial power profile for each experiment was flat (1.0) across the bundle length. The radial pin power was 0.91 for each of the inner 6-pin and 12-pin rings, and 1.09 for each of the outer 18 pins, Figure 8. The heater pins were modeled as three rings of 6, 12 and 18 pins to capture the radial power distribution.

VIPRE-01 Models

A VIPRE-01 sub-channel model was created for both SP1 and SP2. As this was investigating only the steady state pressure drop of the heater region, only the region between the differential-pressure taps DP16-4 in Figures 2 and 6 were included. The exact axial nodalization was used from the RELAP5 models for SP1 and SP2. An azimuthal symmetry of 1/6 was used for the SP1 and 1/12 for the SP2 models (Figures 4 and 8) resulting in 11 sub-channels and 5 sub-channels for the SP1 and SP2 models, respectively. In addition, a single lumped channel model was created for SP2 to provide an exact comparison to the RELAP5 model.

TEST DESCRIPTION

Standard Problem 2

Initial conditions for the SP2 experiments are presented Table 1. In each experiment the inlet control valve was closed to initiate the test, terminating flow to the channel and thus simulating the loss of flow that would occur following a large header rupture. After flow stoppage, liquid in the heater region begins a rapid boil-off and/or liquid expulsion. Within several seconds of valve closure, dryout occurs in the heater bundle and a rapid temperature excursion ensues. As the heater temperature approaches the heater rod design temperature limits, the inlet valve is reopened. The temperature excursion is thus terminated and quenching of the heater bundle occurs. Tests 4, 5, 6, 7 and 8 maintained constant heater power, and test 5′ used a variable heating

rate to simulate reactor shutdown. Test-8 was excluded from this study because the differential pressure measurement was not available.

Standard Problem 1

Initial conditions for the SP1 experiments are presented Table 2. In each experiment the inlet control valve was closed to initiate the test, terminating flow to the channel and thus simulating the loss of flow that would occur following a large header rupture. After flow stoppage, liquid in the heater region begins a slow boil-off and reaches a quasi-steady state condition with liquid drainback (counter-current flow) from the upper piping. Eventually dryout occurs in the heater bundle and a rapid temperature excursion ensues, at which time the experiment is terminated. The reflood portion of these experiments was not investigated, only the time to dryout.

DISCUSSION OF THE INITIAL RESULTS

Standard Problem 2

The predicted error in steady state differential pressure across the entire bundle is presented in Figure 10 for the SP2 base case results. This assumed a wall roughness of drawn tubing (1.5e-6m) and used the default bundle interfacial drag model in RELAP5 (the EPRI model) and the HTFS two-phase multiplier model. The predicted error increases smoothly, from –24% to +9%, when plotted against $\Delta h/h_{fg}$ (change in bundle exit enthalpy divided by heat of vaporization). Attempted variations in the wall roughness did not produce a significant improvement in the predicted error, only a shift in the curve. Using a higher wall roughness (2.5e-5m) yielded an error range of –14% to +27% in the calculated error. In addition the Bestion bundle friction model in RELAP5 was investigated, and yielded a similar steady state error prediction to the EPRI model (not shown as this was within 1% of the EPRI result). However, this similarity would be expected at these high mass flux levels. At high mass fluxes, the measured differential pressure is dominated by wall friction and not interfacial drag and void distribution. The moisture content in the bundle contributes ~17% of the steady-state pressure differential for Test-4, decreasing to less than 5% for Test-7 (including the lower subcooled regions).

Standard Problem 1

The predicted error in steady state differential pressure across the entire bundle is presented in Figure 11 for the SP1 base case results. This assumed a wall roughness of drawn tubing (1.5e-6m) and used the default bundle interfacial drag model in RELAP5 (the EPRI model) and the HTFS two-phase multiplier model. The predicted error varies more randomly, from ~0% to -14%, when plotted against $\Delta h/h_{fg}$. Attempted variations in the wall roughness did not produce a significant improvement in the predicted error. Using a higher wall roughness (2.5e-5m) yielded an error curve only ~1% different (higher). The Bestion bundle friction model was investigated, and yielded a similar steady state error range, however, the curve was shifted upward to –6% to +6 %. This effect would be expected at the SP1 lower mass fluxes, as the moisture content in the heater bundle is now a significant contribution to the total pressure drop, making the differences in interfacial drag significant between the EPRI and Bestion correlations. The moisture content in the bundle contributes ~90% of the steady-state pressure differential for SF-96, decreasing to ~66% for SF-257. This lead to an initial conclusion that the pressure drop error was likely due to void distribution and not friction losses.

STUDY OF THE TWO-PHASE MULTIPLIERS

The RELAP5 and VIRPE codes both use the Lockart-Martinelli method for calculating two-phase pressure drops. R.W. Lockhart and R.C. Martinelli first presented a two-phase multiplier correlation in 1949 [8]. The basis for their correlation was derived from previous studies in 1944-1946 by Martinelli, et. al. [9,10]. In these studies it was demonstrated that the two-phase flow pressure loss could be characterized by four types of flow mechanisms existing during the simultaneous flow of a liquid and a gas or vapor. These mechanisms were identified as:

1. Turbulent flow of both the liquid and vapor - turbulent-turbulent flow (tt)
2. Viscous liquid flow and turbulent vapor flow - viscous-turbulent flow (vt)
3. Turbulent liquid flow and viscous vapor flow - turbulent-viscous flow (tv)
4. Viscous flow of both the liquid and vapor - viscous-viscous flow (vv)

Essentially, the two-phase flow regimes could be characterized by the dimensionless Reynolds number (Re), where turbulent flow was defined as Re > 2000 and viscous flow as Re <2000. The results of those studies demonstrated that the two-phase pressure drop per unit length in each of the flow types could be characterized by (1). This is what is generally considered the Lockhart-Martinelli two-phase multiplier correlation (LM hereafter).

$$(\Delta P/\Delta L)_{tp} = \Phi_g^2 * (\Delta P/\Delta L)_g \qquad (1)$$

where

$$(\Delta P/\Delta L)_{tp} \qquad (2)$$

is the two-phase pressure drop per unit length, and

$$(\Delta P/\Delta L)_g \qquad (3)$$

is the pressure drop per unit length which would exist if only the vapor phase existed in the pipe.

The parameter Φ_g was defined as the two-phase multiplier and was further defined as a function of the dimensionless variable, X. The parameter X was shown to be a function of the ratios of the weight rates of the liquid and vapor, the ratio of the liquid and vapor densities, the ratio of the liquid and vapor viscosities, and the diameter of the pipe. The relationship of the these ratios was easily recognized as being simply the ratio of the liquid and vapor pressure drops, leading to the following definition for X:

$$X^2 = (\Delta P/\Delta L)_l / (\Delta P/\Delta L)_g \qquad (4)$$

Although both codes use the LM correlation (1) to define the multiplier, the actual methodologies vary significantly. This is driven by the fundamental differences between the two codes. The RELAP5 code uses the LM relationship and Chisholm's derivation for Φ_l (as opposed to Φ_g). Chisholm defined the two-phase multiplier using the liquid phase as the reference [11].

$$\Phi_l^2 = 1 + C/X + 1/X^2 \qquad (5)$$

In RELAP5, a correlation is used for C derived by Chaxton, et al. [12]. Chaxton derived C empirically as a function of mass flux (G), phase density ratio (ρ_g / ρ_l), and phase viscosity ratio

(μ_l / μ_g) to improve the accuracy of the two-phase multiplier. The overall relationship is referred to as the HTFS two-phase multiplier in RELAP5.

HTFS (eqs. 6-10):

(6) $C = -2 + f * T$

(7) $f = 28.0 - 0.3 * G^{0.5}$

(8) G = mass flow rate / area, (kg/m^2 sec)

(9) $T = \exp[-(\log(\Lambda) + 2.5)^2 / (2.4 - G/10000)]$

(10) $\Lambda = (\rho_g / \rho_l) (\mu_l / \mu_g)^{0.2}$

For the evaluation of X, and thus the two-phase pressure drop, RELAP5 uses the individual liquid and vapor velocities (11) and (12) to solve the single-phase pressure loss equations for (5).

(11) $\Delta P_l = (f_l L/D) [(1 - \alpha) \rho_l (vel_f)]^2 / 2$

(12) $\Delta P_g = (f_g L/D) [(\alpha) \rho_g (vel_g)]^2 / 2$

The RELAP5 two-phase pressure loss is then calculated similar to (1), except that the liquid phase definition is used instead of the vapor phase for the single-phase pressure loss (13), and then using Φ_l from (5) and C from (6).

(13) $(\Delta P)_{tp} = \Phi_l^2 * (\Delta P)_l$

The VIPRE code (default) uses a correlation for Φ_l developed at Columbia University under EPRI sponsorship [13]. The solution of Φ_l is divided over two pressure ranges and includes the vapor quality (x) and reduced pressure (P / P_{crit}) to improve accuracy.

EPRI (eqs. 14-16):

(14) $\Phi_l^2 = 1 + (\rho_l / \rho_g - 1) C_F$

(15) $C_F = 1.02 (x)^{-0.175} G^{-0.45}$, for $P \geq 600$ psi)

(16) $C_F = 0.357 (x)^{-0.175} G^{-0.45}(1 + 10P / P_{crit})$, $P < 600$ psi)

VIPRE then uses the total mass flow rate of the channel (liquid + vapor) and the liquid density.

(17) $\Delta P = (f_{tp} L/D) G_{tot}^2 / (2 \rho_l)$

(18) $(\Delta P)_{tp} = \Phi_l^2 * \Delta P$

In addition to the default RELAP5 (HTFS) and VIPRE (EPRI) two-phase multipliers, the Friedal, Beattie and a simplified sonic velocity relationship were investigated. All three relationships were based on the total mass flux approach as in VIPRE, (17) and (18). The Beattie correlation is divided into four flow regimes; bubbly, slug, annular and post critical heat flux. In RELAP5 these correspond to flow regimes 4 (bubbly), 5 (slug), 6 and 7 (annular/mist), and 8, 9, 10 and 11 for the post critical heat flux. The additional correlations investigated are given below.

Friedal (eqs. 19-23):

(19) $\Phi_l^2 = A1 + 3.21 * A2 / (Fr^{0.0454} * We^{0.035})$

(20) $A1 = (1 - x)^2 + x^2 * (\rho_l / \rho_g) * (f_g / f_l)$

(21) $A2 = x^{0.78} * (1 - x)^{0.224} * (\rho_l / \rho_g)^{0.91} * (\mu_g / \mu_l)^{0.19} * (1 - \mu_g / \mu_l)^{0.70}$

(22) $Fr = G^2 / (g * D * \rho_{tp}^2)$

(23) $We = G^2 * D / (\rho_{tp} * \sigma)$

Beattie (eqs. 24-27):

(24) $\Phi bubb^2 = (1 + x*(\rho_l / \rho_g - 1))^{0.8} * (1 + x * ((3.5\mu_g + 2.0\mu_l) * \rho_l) / (\rho_g * (\mu_g + \mu_l) - 1))^{0.2}$

(25) $\Phi slug^2 = (1 + x*((\rho_l / \rho_g) - 1))^{0.8} * (1 + x * (3.5 * (\rho_l / \rho_g) - 1))^{0.2}$

(26) $\Phi ann^2 = (1 + x*((\rho_l / \rho_g) - 1))^{0.8} * (1 + x * ((\rho_l / \rho_g)(\mu_g / \mu_l) - 1))^{0.2}$

(27) $\Phi post^2 = (1 + x*((\rho_l / \rho_g) - 1))^{1.8} * (\rho_g / \rho_l)^{0.8} (\mu_g / \mu_l)^{0.2}$

Sonic (eqs. 28-29):

(28) $\Phi_l^2 = [((1 - x) * af + x*ag) / atp]^{0.70}$

(29) $atp = \{(1 - x)*vl + x*vg) / ((1-x)*vl^2 / af^2 + x*vg^2 / ag^2)^{0.5}$

Prior to implementing the code changes into RELAP5, a comparison of the multipliers was made. This was accomplished by stripping calculation results from the base SP2 RELAP5 results as well as the VIPRE calculations for the SP2 lumped (single) channel model. The different correlations were programmed into a spreadsheet (MathCad) and calculations performed to estimate the potential impact in RELAP5. A comparison of the two-phase multipliers versus quality is shown in Figures 12a-12c for SP2 Test-6 (the other cases show similar behavior). These plots are made versus quality, void fraction and node, respectively. Although the RELAP5 calculated multiplier appears to behave differently from the ERPI (designated VIPRE) and Friedal correlations, this is because of the reference definition for the single-phase pressure drop. If the RELAP5 multiplier is converted to a total mass flux definition, then the multipliers behave similar. The Beattie correlation shows a drop in the multiplier when the flow regime changes from slug to annular (at node 30, Figure 12c). The sonic multiplier shows a higher value in the low quality region (which would be slug flow) and decreasing slowly in the annular flow regime. Figure 12b shows the nearly symmetrical behavior of the sonic multiplier.

Although the actual parameters for velocities, void fraction, etc. would change for each correlation when implemented, the comparison indicates that the Friedal and EPRI correlations should over-predict the bundle pressure drop compared to the HTFS, while the Beattie correlation would under-predict the pressure drop. The sonic multiplier would appear to dramatically under-predict the pressure drop.

The RELAP5 code contains only the HTFS two-phase multiplier and so the code was recompiled to include the different correlations. The VIPRE code contains both the EPRI and Beattie multipliers (with EPRI as the default choice). The VIPRE code was used only with the two available correlations (no code modifications were attempted). The RELAP5 code was modified to include the Friedal, Beattie and sonic based multipliers. Each correlation was implemented separately and a new code version compiled. The modifications were done in the fwdrag subroutine where the HTFS multiplier is calculated in RELAP5. The coding as implemented is presented in Appendix A (changes to fwdrag). The Friedal and Beattie correlations were already consistent with the metric units used in RELAP5, however, the EPRI correlation required conversion of the mass flux from British units. Also, the reference basis of the multipliers in RELAP5 was modified to the total mass flux (although the two-phase partitioning scheme was

not modified). This is shown below (and in Appendix A). The two-phase definition for 'tpdpdx' was commented out, and replaced with a total mass flux based definition. The term 'dpdxff' replaces the calculation for 'dpdxfx' in fwdrag (below). For simplicity, arrays were not set up for the modifications.

```
            gfwsq = gfwabs(ix) * gfqabs(ix)
            dpdxff = gfwsq/rhof(i)*(frlmf1(ix) + frtrf1(ix)*(frtbf1(ix) - frlmf1(ix)))
            tpdpdx(ix) = dpdxff*(multiplier from Friedal, EPRI, Beattie, or sonic)
c-----------------------------------------------------------------
c           tpdpdx(ix) = dpdxfx(ix) + dpdxgx(ix) +
c    &      ctermx(ix)*sqrt(dpdxfx(ix)*dpdxgx(ix))
```

The 'dpdxfx' term as defined in RELAP5 is below, and is replaced by dpdxff from above in the definition for 'tpdpdx'.

```
            dpdxfx(ix) = rhof(i)*axvelf(ih1)*axvelf(ih1)*
     &       (frlmf1(ix) + frtrf1(ix)*(frtbf1(ix) - frlmf1(ix)))
```

RESULTS

VIPRE-01

The VIPRE-01 code was used primarily to determine if sub-channel effects could account for the discrepancies seen in the steady state pressure drop across the bundle. The SP2 results for the EPRI and Beattie two-phase multipliers, and sub-channel and lumped models, are shown in Figure 13 with the base RELAP5 results also shown. The sub-channel EPRI results show a narrower error range, however, the error curve exhibits similar characteristics for the increase in pressure drop error as in RELAP5. The lumped channel EPRI results show an upward shift in the error curve (increase in pressure drop), but the same error curve characteristics. This would indicate that a lumped model should tend to over-predict the two-phase pressure drop, but that sub-channel effects are not significant relative to the systematic error in the two-phase pressure drop calculation. The Beattie correlation shows better steady state characteristics, except for Test-4, as the error curve shows a flatter profile for Tests 5, 5', 6 and 7. As with the EPRI results, the lumped model curve is shifted up, but the shape is not changed dramatically.

The SP1 calculations were repeated using the EPRI and Beattie two-phase multipliers and a full sub-channel model (no lumped model was created for SP1). These results are shown in Figure 14. The EPRI error range is smaller the RELAP5 results, -1% to –10%, and shifted slightly up. The Beattie results are shifted lower, with a slightly larger error range, -4% to –22%. However, the same characteristic behavior is seen in the calculated pressure drop error as in RELAP5.

RELAP5

The RELAP5 code was modified to include the Friedal, EPRI, Beattie and sonic two-phase multipliers. The coding added to subroutine fwdrag is shown in Appendix A for each correlation. The SP2 results are shown in Figure 15. As expected, the Friedal correlation yielded a slightly higher pressure drop, shifting the error curve up, and the Beattie correlation slightly lower, shifting the error curve down. The error characteristics, however, were the same. Increasing the wall roughness to 2.5e-5m with the Beattie correlation shifted the curve up, as expected, but did not alter the shape. The EPRI correlation significantly under-predicted the pressure drop, shifting

the curve down, but did flatten the error curve slightly. Increasing the wall roughness to 2.5e-5m with the EPRI correlation shifted the curve up, as expected, but did not alter the shape. The sonic correlation, unexpectedly, yielded the best results using the default wall roughness of 1.5e-6m.

The SP1 cases were then re-calculated and the results are shown in Figure 16. The Friedal, EPRI and Beattie correlations each behaved similar to the base RELAP5 (HTFS) calculations. The EPRI and Beattie correlations yielded slightly lower curves, while the Friedal correlation nearly reproduced the HTFS results. The sonic correlation yielded a slightly higher pressure drop, shifting the error curve upward, with a larger relative change for the lower power cases.

Additional Insight

Regardless of the correlation used, the calculated pressure drop error curve all exhibited similar characteristics (systematic error). In reviewing the calculation results one consistency was seen between both the SP1 and SP2 results. This was related to the calculated drift velocity. In SP1, test cases SF-96, SF-161, SF-202, and SF-257 had similar maximum drift velocities (vgjj ~0.091m/s) and the remaining cases about 10% lower (~0.084m/s). This is shown Figure 17, which connects the calculations by approximately constant, maximum drift velocities for the base RELAP5 (this is consistent in all of the calculations). For SP2, Test-4 yields the highest maximum drift velocity (0.084m/s), with each subsequent case yielding lower values. Test-5 is 0.064m/s and Tests 5', 6 and 7 are at 0.048m/s. This would indicate that the two-phase pressure drop is showing a dependency on the drift velocity, or slip, that is not currently accounted for.

CONCLUSIONS

1) The results of the VIPRE-01 calculations indicate that the error dependency in the two-phase bundle pressure for SP1 and SP2 is not a sub-channel issue. The total pressure loss calculated was dependent on the lumped versus sub-channel configuration and the two-phase multiplier correlation. However, the pressure drop error characteristics were identical.
2) The existing correlations of Friedal, EPRI and Beattie, did not provide significant improvement over the HTFS in the calculated steady state pressure drop error for SP1 and SP2.
3) The error characteristics indicate a potential dependency on the drift velocity. This was seen in both SP1 and SP2. That is, the higher the drift velocity, the lower the calculated pressure drop compared to the data.
4) The sonic velocity based correlation, unexpectedly, gave improved characteristics for the SP2 cases for the steady state solutions. Although the results are intriguing, no basis is provided for why this 'may' have worked for SP2. This may indicate that the choke flow models could provide an improved two-phase multiplier correlation (for vertical flow in a bundle). The SP1 results showed similar behavior as the HTFS, EPRI, Friedal, and Beattie correlations.
5) The transient behavior of the different two-phase multipliers must be investigated.
6) Additional review of the two-phase pressure drop database is needed to compare where the RBMK experimental data resides. Clearly, the fact that the axial void distribution is not constant in the experiments and that both slug and annular two-phase flow regimes exist complicates whether either regime is being calculated correctly.

REFERENCES

1) RELAP5/MOD3 Code Manual, NUREG/CR-5535, Vols. 1-5, 1995.
2) "RBMK SP-2 Validation Results (KS PH Rupture Simulation)," paper presented at the 6th International Exchange Forum, Kiev, Ukraine, 2002.
3) VIPRE-01 Code Manual, EPRI NP-2511-CCM-1, Vols. 1-3, 1989.
4) Friedal, L., "Improved Friction pressure Drop Correlations for Horizontal and Vertical Two-Phase Flow," Paper E2, presented at the European Two Phase Flow Group Meeting, Ispara, Italy, 1979.
5) Joint Project 6, "Definition Report for INSCSP-R1," 1998.
6) Joint Project 6, "Comparison Report for INSCSP-R1," 1999.
7) "RBMK Type Reactor Core Thermal Hydraulic Processes Investigation Under Pressure Header Break Conditions ", Standard Problem INSCSP-R2 Definition, 1998.
8) Lockhart, R.W. and Martinelli, R.C., University of California, Berkeley, "Proposed Correlation of Data for Isothermal Two-Phase, Two-Component Flow in Pipes," *Chemical Engineering Progress*, January, 1949, Vol. 45, No. 1.
9) Martinelli, R.C, Boelter, L.M.K., Taylor, T.H.M., Thomsen, E.G, and Morrin, E.H., *Trans. Am. Soc. Mech. Engrs.*, 66, 2, 139-52, 1944.
10) Martinelli, R.C, Putnam, J.A. and Lockhart, R.C., *Trans. Am. Inst. Cem. Engrs.*, 42, 4, 681, 1946.
11) Chisholm, D., National Engineering Laboratory, "A Theoretical Basis for the Lockhart-Martinelli Correlation for Two-Phase Flow," *Int. J. Heat Mass Transfer*, Vol. 10, pp 1767-1778, 1967.
12) Chaxton, K.T., Collier, J.G, and Ward, J.A., "H.T.F.S. Correlation for Two-Phase Flow Pressure Drop and Void Fraction in Tubes," UK, AERE-R7162, 1972.
13) Reddy, D.G., et al., "Two-Phase Friction Multiplier for High Pressure Steam-Water Flow," EPRI-NP-2522, 1982.

DEFINITIONS

af – liquid phase sonic velocity
ag – vapor phase sonic velocity
atp – two-phase mixture sonic velocity
D – volume hydraulic diameter (4*area/wetted perimeter)
f_{tp} – two-phase friction factor
f_l – liquid-phase friction factor
f_g – vapor-phase friction factor
G – mass flux
L – volume node length
P – pressure
Pcrit – critical pressure
vel_f – liquid velocity
vel_g – vapor velocity
vl – liquid specific volume
vg – vapor specific volume
x – vapor quality
$(\Delta P/\Delta L)_{tp}$ - two-phase pressure drop per unit length
$(\Delta P/\Delta L)g$ – vapor phase only pressure drop per unit length
$(\Delta P/\Delta L)g$ – liquid phase only pressure drop per unit length
Φ_g^2 - two-phase multiplier based on vapor phase only pressure drop
Φ_l^2 - two-phase multiplier based on liquid phase only pressure drop
ρ_g – vapor density
ρ_l – liquid density
μ_l – liquid viscosity
μ_g – vapor viscosity

APPENDIX A – RELAP5 Code Modifications

EPRI Two-Phase Multiplier

```
c-----------------------------------------------------------------------
c new defintions for epri  correlation
      real cfepri,cfhip,cflop,fcom,gfwsq,dpdxff
c-----------------------------------------------------------------------
c epri based multiplier
            gfwsq = gfwabs(ix) * gfwabs(ix)
         fcom = quals(i)**(-0.175)*(gfwabs(ix)*7.373e-04)**(-0.45)
            cfhip = 1.02*fcom
            cflop = 0.357*fcom*(1.0 + 10.0*p(i)/2.212e+07)
            if(p(i) .lt. 4.137e+06) then
              cfepri = cflop * quals(ix)
             else
              cfepri = cfhip * quals(ix)
            endif
            dpdxff = gfwsq/rhof(i)*
     &        (frlmf1(ix) + frtrf1(ix)*(frtbf1(ix) - frlmf1(ix)))
          tpdpdx(ix) = dpdxff*(1.0+(rhof(i)/rhog(i)-1.0)*cfepri)
c-----------------------------------------------------------------------
c             tpdpdx(ix) = dpdxfx(ix) + dpdxgx(ix) +
c    &        ctermx(ix)*sqrt(dpdxfx(ix)*dpdxgx(ix))
c-----------------------------------------------------------------------
```

Friedal Two-Phase Multiplier

```
c-----------------------------------------------------------------------
c new defintions for Friedal correlation
      real fra1,fra2,dpdxff,froude,weber,rhorat,frcrat,gfwsq,vscrat
c-----------------------------------------------------------------------
c Friedal correlation
c The Fr corr. is based on dpdx being calculated from gfwabs**2/rho
c and not as RELAP5 calculates it above, "rho*axvel*axvel". Therefore,
c a gfwabs based dpdx is added so that tpdpdx is correctely calculated
            rhorat = rhof(i)/rhog(i)
            vscrat = viscg(i)/viscf(i)
            gfwsq = gfwabs(ix)*gfwabs(ix)
            frcrat =
     &        (frlmg1(ix) + frtrg1(ix)*(frtbg1(ix) - frlmg1(ix)))/
     &        (frlmf1(ix) + frtrf1(ix)*(frtbf1(ix) - frlmf1(ix)))
            fra1 = (1.0 - quals(i))*(1.0 - quals(i)) +
     &        quals(i)*quals(i)*rhorat*frcrat
            fra2 = (quals(i)**0.78)*((1.0 - quals(i))**0.224)*
     &        (rhorat**0.91)*(vscrat**0.19)*
     &        (1.0 - vscrat)**0.70
            froude = gfwsq/(9.806*diamv(i+nd)*rhom(i)*rhom(i))
            weber = gfwsq*diamv(i+nd)/(rhom(i)*sigma(i))
```

```
c tpdpdx is based on "dpdxfx*(1+C/X+1/X^2)", so new tpdxfx must incl
c dpdxff term. X is sqrt(dpdxfx/dpdxgx). dpdxff is not set
c up as an array yet, but does not need to be.
            dpdxff = gfwsq/rhof(i)*
     &       (frlmf1(ix) + frtrf1(ix)*(frtbf1(ix) - frlmf1(ix)))
            tpdpdx(ix) = dpdxff*(fra1 + 3.21*fra2/
     &       ((froude**0.0454)*(weber**0.035)))
c-----------------------------------------------------------------------
c             tpdpdx(ix) = dpdxfx(ix) + dpdxgx(ix) +
c    &        ctermx(ix)*sqrt(dpdxfx(ix)*dpdxgx(ix))
c-----------------------------------------------------------------------
```

Beattie Two-Phase Multiplier

```
c-----------------------------------------------------------------------
c new defintions for beattie correlation
      real gfwsq,dpdxff,rhorat,vscrat,bubtp,slgtp,anntp,psttp,tpmult,
     &     fcom
c-----------------------------------------------------------------------
c beattie two-phase multiplier
            gfwsq = gfwabs(ix)*gfwabs(ix)
            rhorat = rhof(i)/rhog(i)
            vscrat = viscg(i)/viscf(i)
            tpmult = 1.0
            fcom  = (1.0 + quals(i)*(rhorat - 1.0))**(0.8)
c bubble flow regime multiplier (4)
            bubtp = fcom *
     &       (1.0 + quals(i)*((3.5*viscg(i) + 2.0*viscf(i)) /
     &       (viscg(i) + viscf(i)) * rhorat - 1.0))**(0.2)
c froth/slug flow regime multiplier (5)
            slgtp = fcom *
     &       (1.0 + quals(i)*(3.5 * rhorat - 1.0))**(0.2)
c annular flow regime multiplier (6,7)
            anntp = fcom *
     &       (1.0 + quals(i)*(vscrat * rhorat - 1.0))**(0.2)
c post chf flow regime multiplier (8,9,10,11)
            psttp = fcom**(1.8) *
     &       vscrat**(0.2) / rhorat**(0.8)
c select multiplier
c flow regime 4 - bubbly
      if((floreg(i).gt.3.5).and.(floreg(i).lt.4.5)) then
         tpmult = bubtp
      else
c flow regime 5 - slug
         if((floreg(i).gt.4.5).and.(floreg(i).le.5.5)) then
            tpmult = slgtp
         else
c flow regime 6,7  - annular/mist
            if((floreg(i).gt.5.5).or.(floreg(i).lt.7.5)) then
               tpmult = anntp
```

```
            else
c flow regime 9,10,11 - post chft
                if((floreg(i).ge.8.0).and.(floreg(i).le.11.0))
     &            then
                  tpmult = psttp
                else
                endif
              endif
            endif
          endif
              dpdxff = gfwsq/rhof(i)*
     &         (frlmf1(ix) + frtrf1(ix)*(frtbf1(ix) - frlmf1(ix)))
              tpdpdx(ix) = dpdxff*tpmult
c-----------------------------------------------------------------------
c             tpdpdx(ix) = dpdxfx(ix) + dpdxgx(ix) +
c    &         ctermx(ix)*sqrt(dpdxfx(ix)*dpdxgx(ix))
c-----------------------------------------------------------------------
```

Sonic Two-Phase Multiplier

```
c-----------------------------------------------------------------------
c new defintions for sonic correlation
      real sonrat,sndf,sndg,gfwsq,dpdxff
c-----------------------------------------------------------------------
c sonic velocity based multiplier (sound eq OK for 4-8 MPa)
              gfwsq = gfwabs(ix)*gfwabs(ix)
              sndf = 1144.2 - 4.7366e-05 * p(i)
              sndg = 478.35 - 8.820e-06 * p(i)
              sonrat = (((1.0 - quals(i))*sndf + quals(i)*sndg)/
     &           sounde(i))
              dpdxff = gfwsq/rhof(i)*
     &           (frlmf1(ix) + frtrf1(ix)*(frtbf1(ix) - frlmf1(ix)))
              tpdpdx(ix) = dpdxff*sonrat**(0.7)
c-----------------------------------------------------------------------
c             tpdpdx(ix) = dpdxfx(ix) + dpdxgx(ix) +
c    &         ctermx(ix)*sqrt(dpdxfx(ix)*dpdxgx(ix))
c-----------------------------------------------------------------------
```

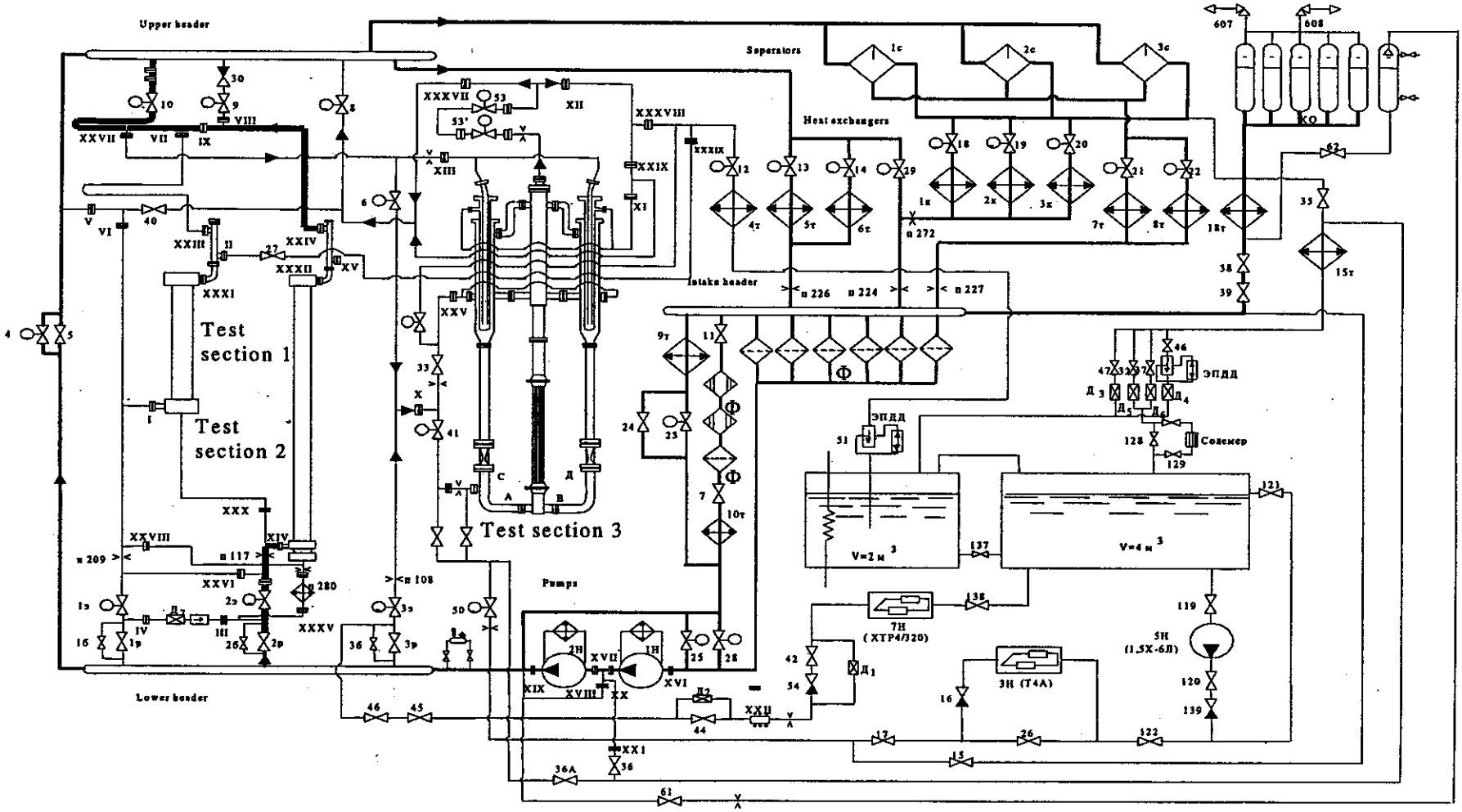

Figure 1) Schematic of the KS Facility

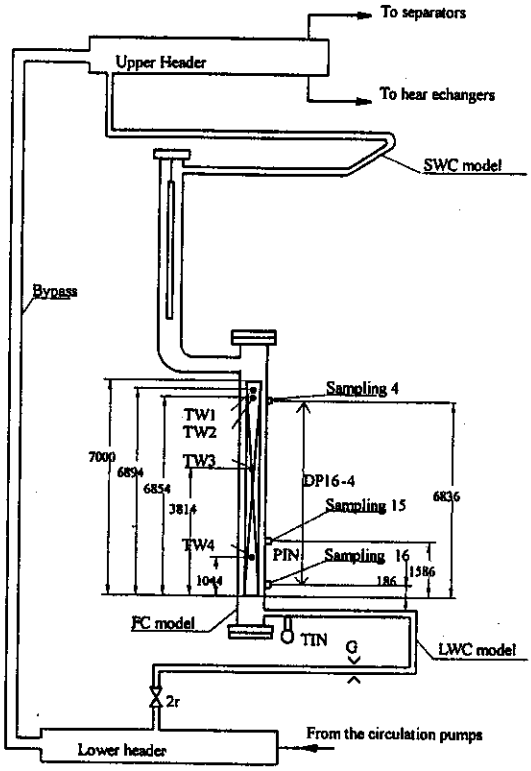

Figure 2) SP2 Test Section 2

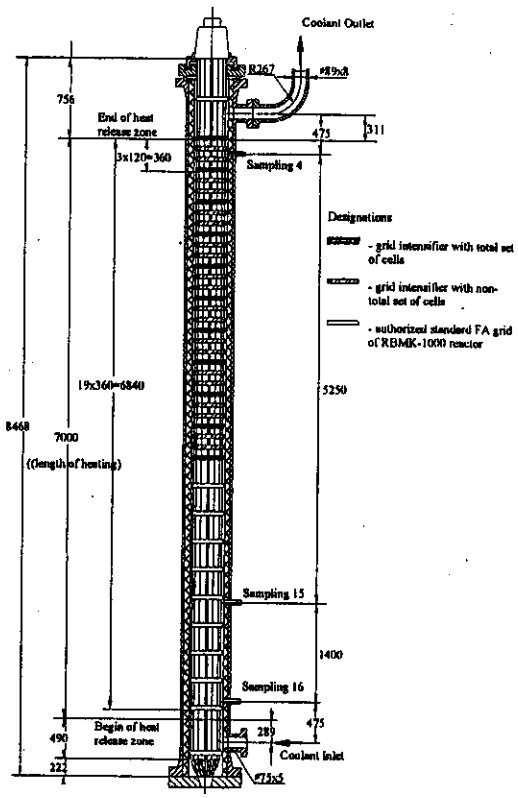

Figure 3) SP2 Heater Bundle Details

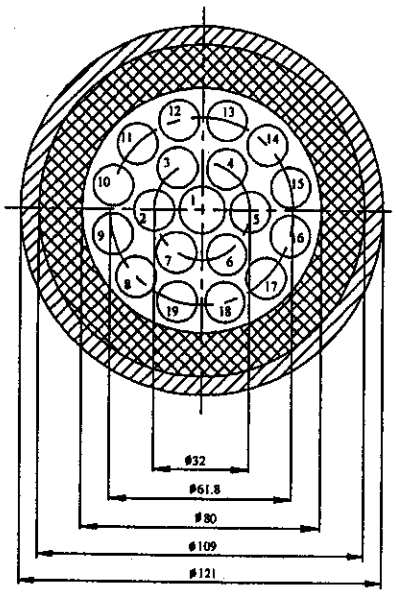

Figure 4) SP2 Heater Bundle Cross-Section

Figure 6) KS Model Node Diagram

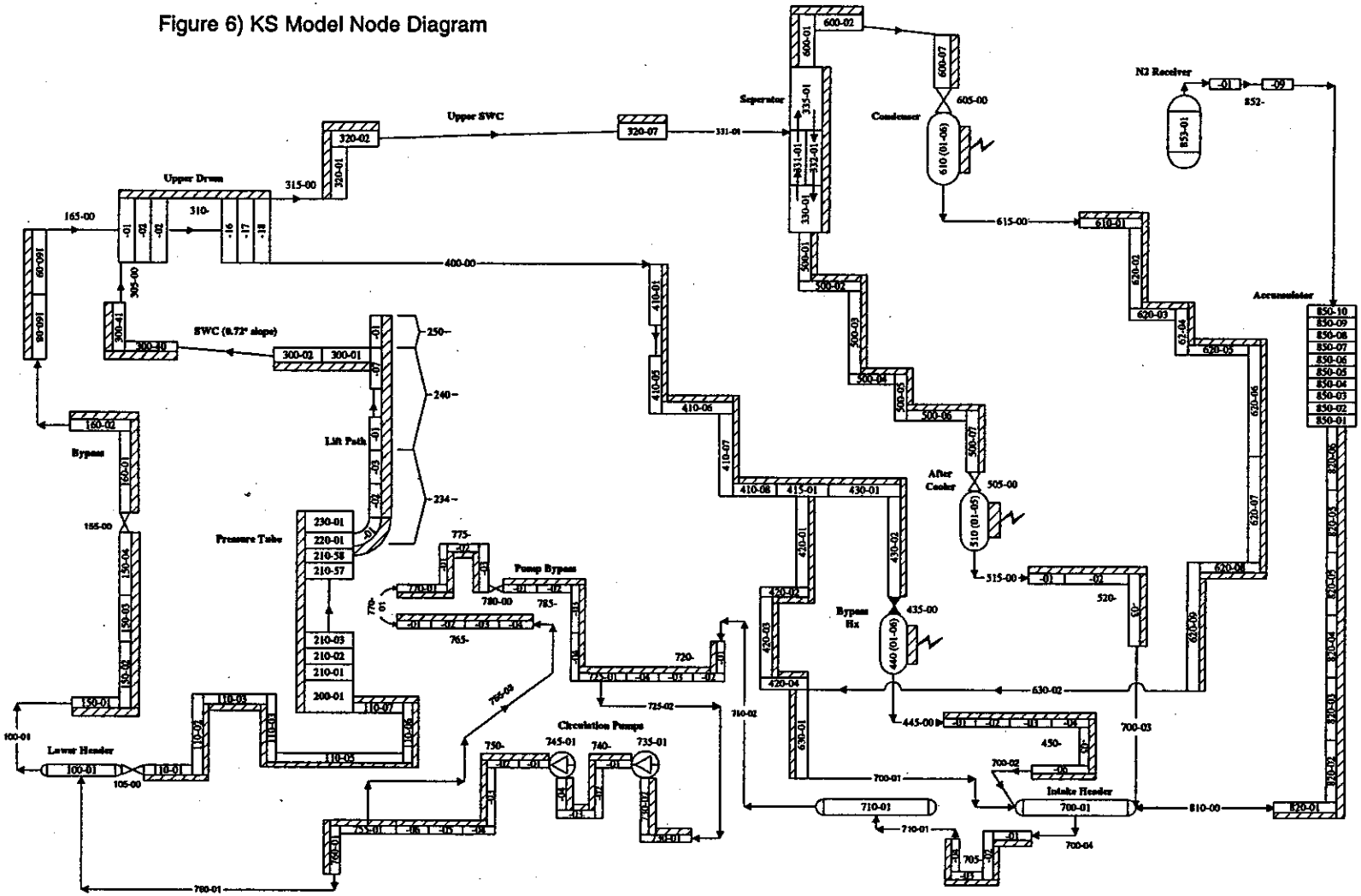

Figure 5) SP2 RELAP5 Model Nodalization

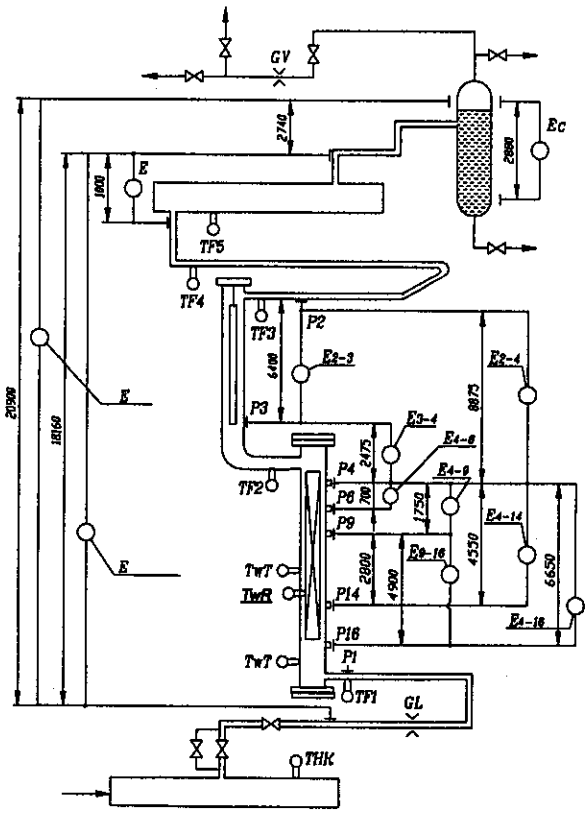

Figure 6) SP1 Test Section 2

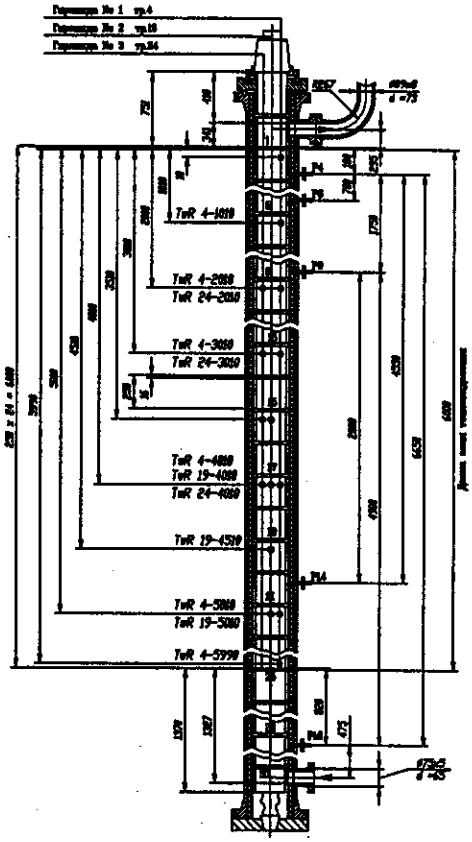

Figure 7) SP1 Heater Bundle Details

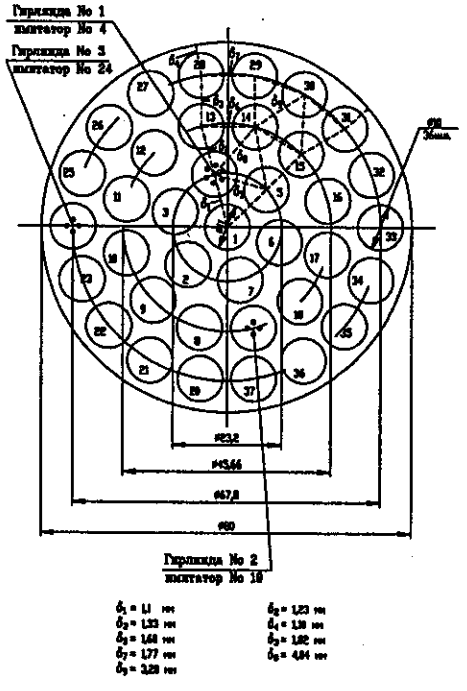

Figure 8) SP1 Heater Bundle Cross-Section

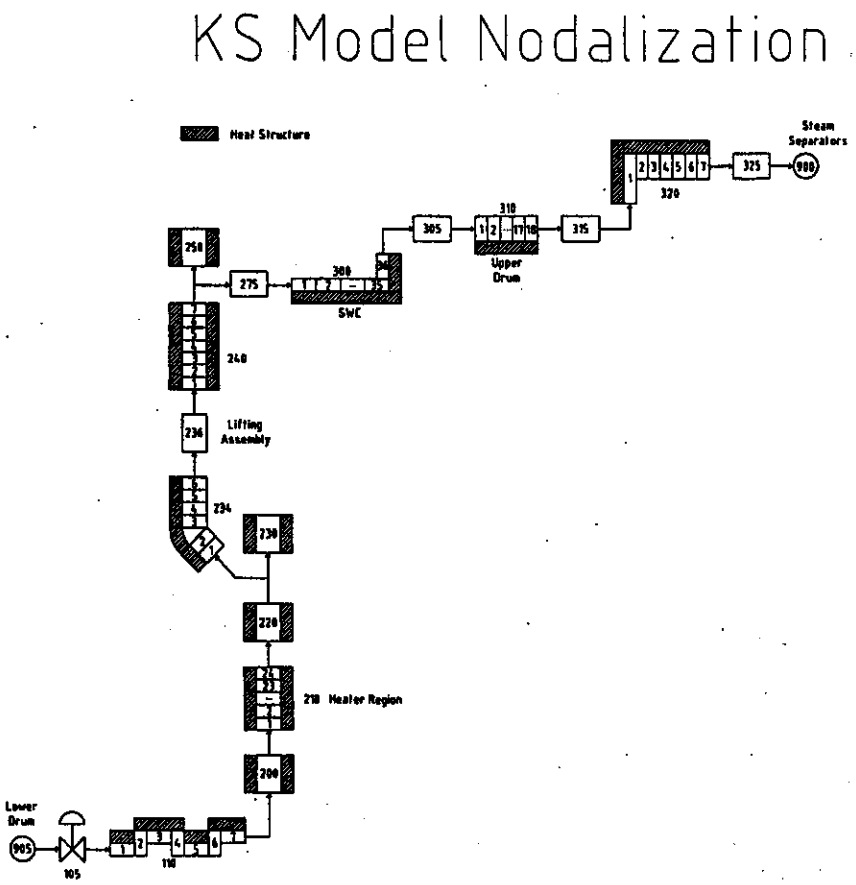

Figure 9) SP1 RELAP5 Model Nodalization

Figure 10) RELAP5 HTFS Results for SP2

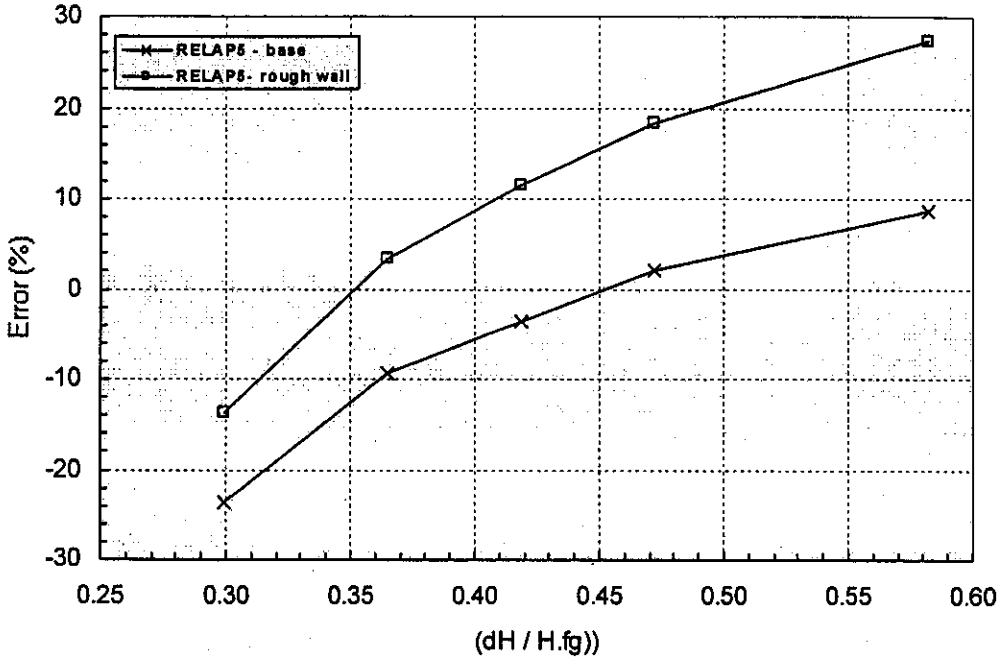

Figure 11) RELAP5 HTFS Results for SP1
(HTFS and different bundle friction)

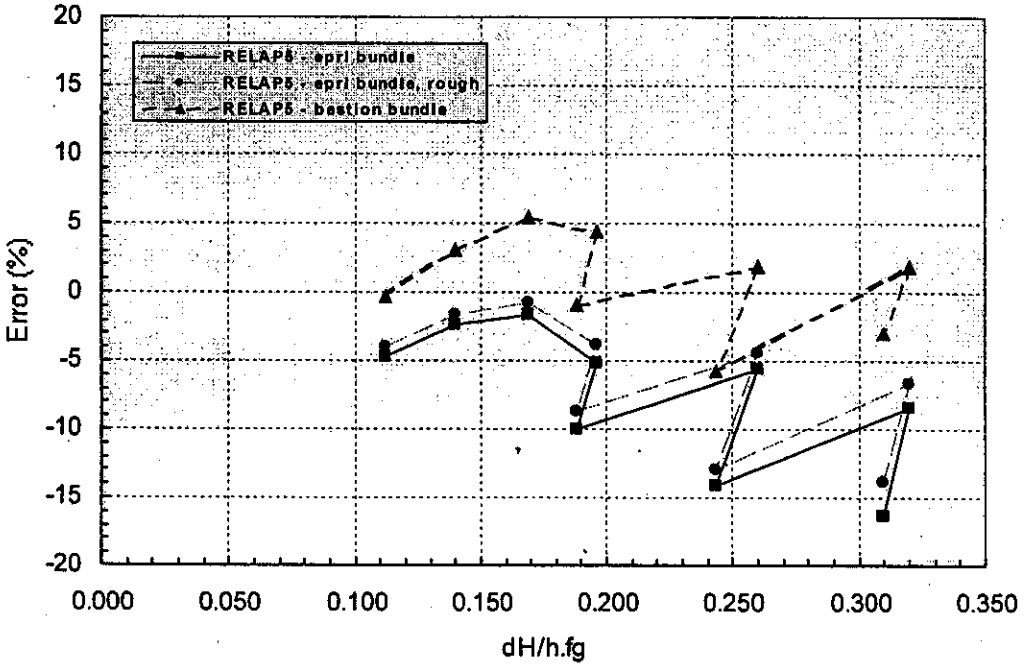

Figure 12a - vs quality

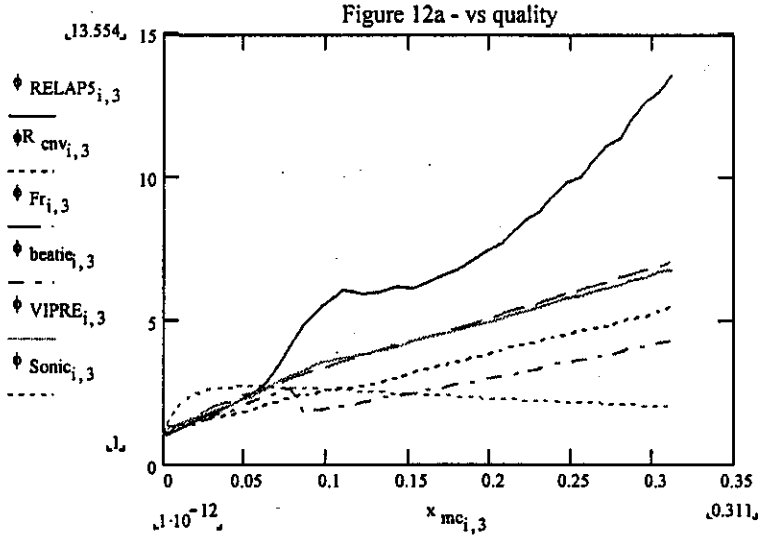

Figure 12b - vs void fraction

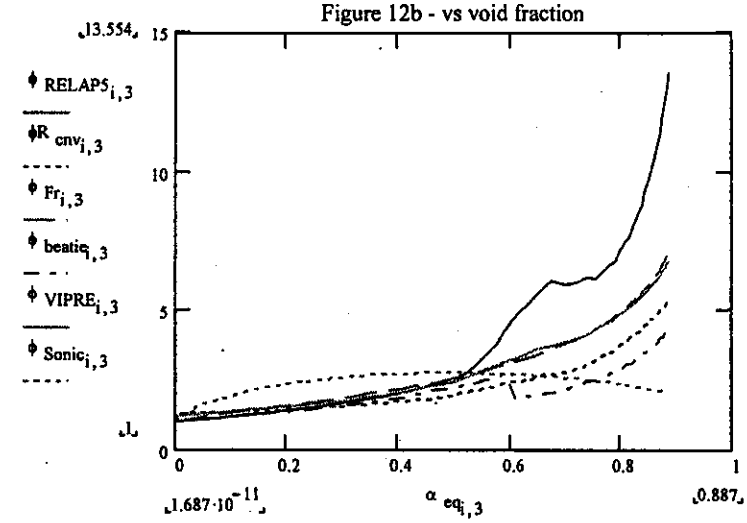

Figure 12c - versus node

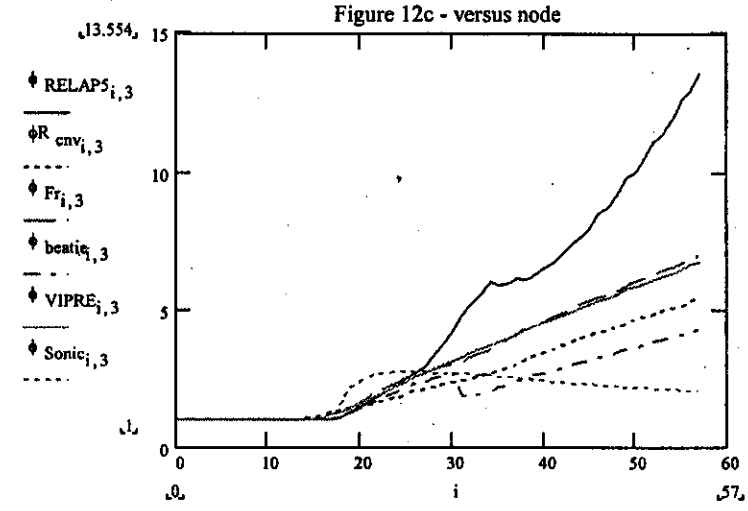

Figure 13) VIPRE Results for SP2

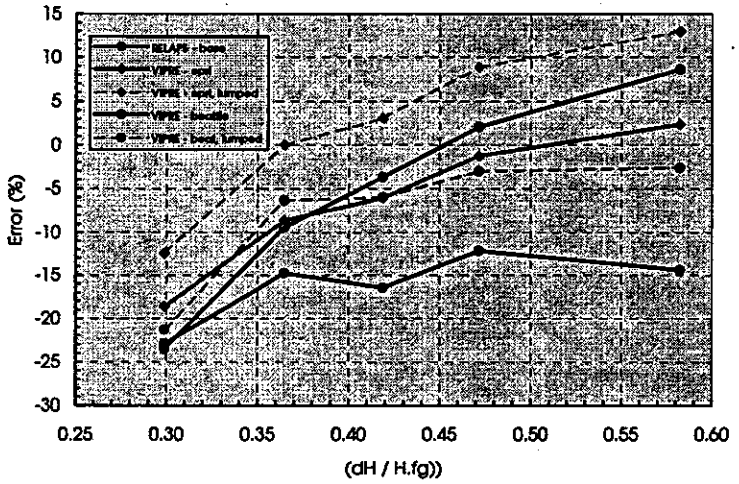

Figure 14) VIPRE Results for SP1
(sub-channel models only)

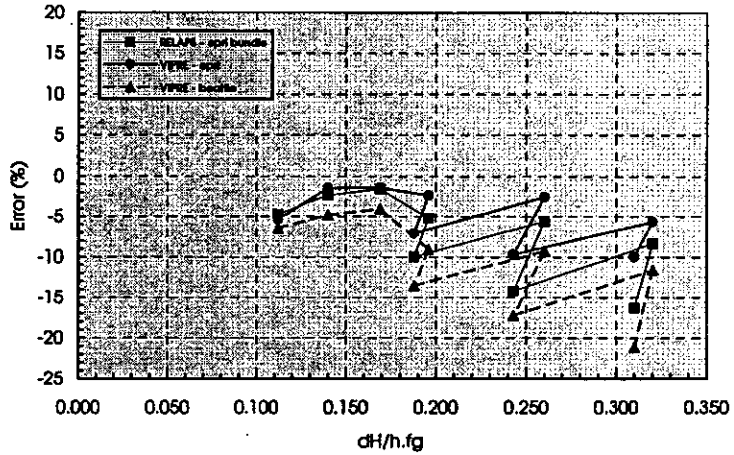

Figure 15) Modified RELAP5 Results for SP2

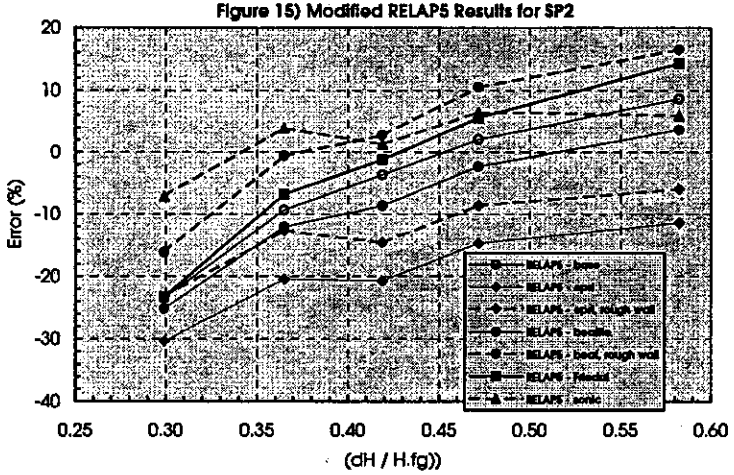

Figure 16) Modified RELAP5 Results for SP1
(EPRI bundle friction model)

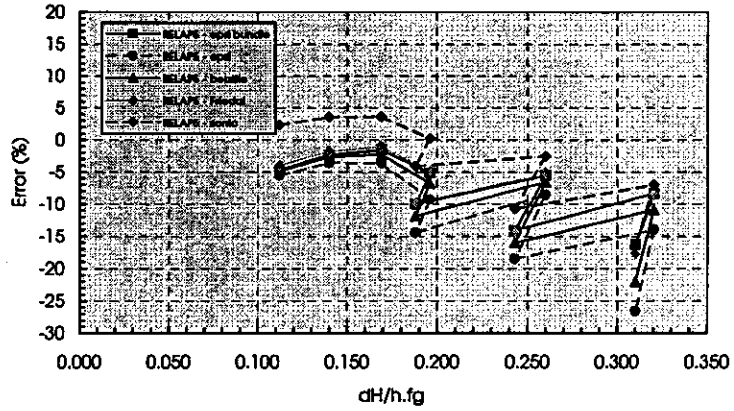

Figure 17) RELAP5 HTFS Results for SP1
(constant lines of drift velocity)